Fano Resonance from Air-mode Photonic Crystal Nanobeam Cavity with 248-nm DUV Lithography

Fujun Sun
Integrated Circuit Advanced Process R&D Center of IMECAS
Institute of Microelectronics, Chinese Academy of Sciences
Beijing, China
sunfujun@ime.ac.cn

Gang Yang
Integrated Circuit Advanced Process R&D Center of IMECAS
Institute of Microelectronics, Chinese Academy of Sciences
Beijing, China
yanggang@ime.ac.cn

Peng Zhang
Integrated Circuit Advanced Process R&D Center of IMECAS
Institute of Microelectronics, Chinese Academy of Sciences
Beijing, China
Zhangpeng1@ime.ac.cn

Bo Tang
Integrated Circuit Advanced Process R&D Center of IMECAS
Institute of Microelectronics, Chinese Academy of Sciences
Beijing, China
tangbo@ime.ac.cn

Zhihua Li
Integrated Circuit Advanced Process R&D Center of IMECAS
Institute of Microelectronics, Chinese Academy of Sciences
Beijing, China
lizhihua@ime.ac.cn

Bin Li
Integrated Circuit Advanced Process R&D Center of IMECAS
Institute of Microelectronics, Chinese Academy of Sciences
Beijing, China
libin1@ime.ac.cn

Yan Yang
Integrated Circuit Advanced Process R&D Center of IMECAS
Institute of Microelectronics, Chinese Academy of Sciences
Beijing, China
yyang@ime.ac.cn

***Abstract*—Photonic crystal nanobeam cavity (PCNC) is important building block for large-scale photonic integrated circuits (PICs). Nevertheless, most state-of-the-art demonstrations rely on electron beam lithography (EBL). Here, we experimentally present the characteristics of Fano resonance from air-mode PCNC using 248-nm deep ultraviolet (DUV) lithography for the first time. Experimentally high average *Q*-factor of ~ 1.58 × 10^4 is achieved.**

Keywords—integrated photonics, nanobeam cavity, DUV

I. INTRODUCTION

In silicon photonics, micro-resonators including micro rings/disks and photonic crystal cavities are important building blocks for large-scale photonic integrated circuits (PICs). Among them, photonic crystal nanobeam cavities (PCNCs) have attracted extensive attention for the investigation of optical sensing, switching, filtering, modulating and lasing, owing to ultra-high quality factor (Q-factor), small mode volume (V), less free spectrum range (FSR) limitation and compact footprint. However, the demanding nature of photonic crystal devices in terms of fabrication capabilities is high. The high lithography resolution such as e-beam lithography (EBL) is required to define the small feature size, which is not practical for manufacturing PICs with large number of components. Therefore, recently several groups worked on the development of dielectric PCNCs [1-3] and 2D photonic crystal devices [4-5] defined using deep ultraviolet (DUV) lithography. However, the feasibility of air-mode PCNC have not been explored yet. Compared with dielectric-mode PCNC, air-mode PCNC confines large electric fields in low refractive index region, which are suggested for the application of refractive index sensing to achieve higher sensitivity. In addition, compared with the usual symmetric Lorentzian resonance line-shape achieved by ordinary side-coupled PCNC structure [6-8], Fano resonance line-shape has steeper asymmetric shape to enable photonic switches and sensors with superior characteristics.

Therefore, in this work, Fano resonances from air-mode PTE-PCNCs fabricated with 248-nm DUV lithography on silicon photonic platform are explored. The results and analysis will contribute to building ultra-compact lab-on-chip resonance-based photonic components such as sensors, switches, filters, reflectors, and so on.

II. DESIGN

Aiming to fabricate the device on a standard full-process complementary metal-oxide-semiconductor (CMOS) passive multi-project-wafer (MPW) run, the device should be designed to comply with the rules defined for this process. The devices are fabricated by 248 nm-λ DUV lithography on SOI wafer with a 3 μm-thick buried oxide (BOX) layer and a 220 nm-thick top-silicon (Si) layer. As part of a MPW run, 2 μm-thick silicon oxide (SiO_2) top-cladding is included in the process flow.

As depicted schematically in Fig. 1(a), Fano resonance occurs from optical interference between the discrete state (fundamental air-mode) of the PCNC and the continuum mode of the side-coupled line-defect waveguide with PTE. The PCNC consists an array of circular holes etched into a Si strip waveguide. The diameter of the holes is $2r$ = 180 nm, which conforms the minimum feature size. The structure is symmetric with respect to the red dashed line shown in Fig. 1(a). The PCNC is optimized using the deterministic high-*Q* design method introduced by Quan et. al [9]. For the tapered region, the hole lattice constant is quadratically tapered from 448 nm in the center to 400 nm on both sides. For the designed PTE-PCNC structure, the PTE is formed by two holes with radius r located in the center of waveguide. The distance d between the two holes in x direction is set as 448 nm, which is the same as the lattice constant of the central tapered segment in PCNC.

Taking N_{taper} = 6 and g = 200 nm for example, the numerical transmission spectra is shown in Fig. 1(b). To make a comparison, the transmission spectra of the line-defect

waveguide with PTE and the ordinary side-coupled cavity without the PTE are also shown. As shown, when there is no PTE, transmission line-shape with Lorentzian symmetric is achieved. The ER (~0.63 dB) is rather low due to the under-coupled condition ($Q_c > Q_r$). While, for PTE-PCNC, a sharper and higher-ER asymmetric Fano line-shape appears in the transmission spectrum, though higher insertion loss ~ 2.22 dB is generated due to the PTE. The corresponding calculated electric field (E) distributions of PTE-PCNC in the xy plane (z = 0) for the modes at wavelength of 1530 nm and 1570 nm are shown in Fig. 1(c). When the waveguide mode is non-resonant with the cavity mode, the light can not be coupled into the cavity and is reflected mostly by the PTE. While, the light with the cavity resonance frequency couples into the cavity and transmits to the output port of the waveguide. Therefore, Fano type peak appears in the transmission spectrum.

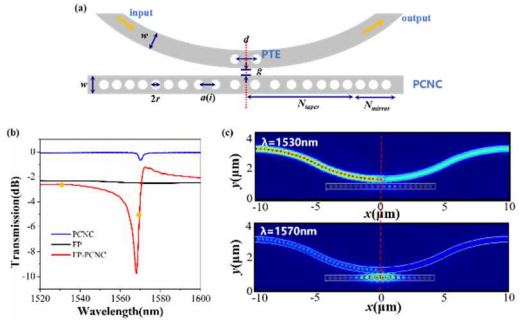

Fig. 1. (a) Schematics of the proposed air mode Fano resonance PTE-PCNC and side-coupling model. The structure is symmetric with respect to its center (black dashed line).

III. Fabrication and Characterization

A. Fabrication

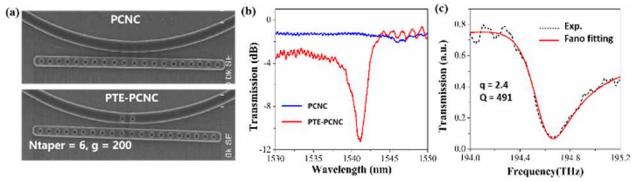

Fig. 2. (a) The SEM images of fabricated side-coupled PCNC without/with PET for N_{taper} = 6 and g = 200 nm. (b) The corresponding measured transmission spectra of the side-coupled cavity without/with PTE. (c) The zoomed in view of the mode, the black dots are the experimental data and the red line shows the Fano fitting.

Our devices were fabricated on an 8-inch SOI wafer with a 220 nm-thick top-silicon layer and a 3 μm-thick BOX in a CMOS pilot line. To realize optical characterization, the waveguides were integrated with TE grating couplers. The DUV photolithography was employed to form the devices patterns on photoresist as a soft mask. Double Inductively coupled plasma (ICP) etching processes were applied to transfer the patterns from the photoresist layer to silicon to form waveguides and devices. 220 nm full etching was defined for waveguides and circle holes, and 70 nm shallow etching was defined for grating lines. The devices were oxide-embedded through oxide deposition by plasma-enhanced chemical vapor deposition (PECVD) and planarization down to the top of the silicon layer. Taking devices with g = 200 nm and N_{taper} = 6 for example, Fig. 2 (a) shows the scanning electron microscope (SEM) images of the fabricated side-coupled PCNC and PTE-PCNC, indicating well-defined circular holes and the coupling region.

B. Characterization

The fabricated devices were characterized by measuring the transmission, using a tunable laser (from 1500 to 1620 nm), and cleaved single-mode fibers for input/output coupling. The transmittances were obtained by normalizing the spectra to a reference waveguide, as shown in Fig. 2 (b). Obviously, the line-shapes correspond well with the simulation results shown in Fig. 1 (b). The fabrication induced roughness (such as imperfect circular holes, rough sidewall and lag effect) may be the reason for the wavelength discrepancy between the simulation and the experimental. As shown in Fig. 2 (b), the coupling between PCNC and waveguide for g = 200 nm makes the measured transmission spectrum of side-coupled PCNC has Lorentzian resonance line-shape with ultra-low ER. To evaluate the Q-factor of the PTE-PCNC, the asymmetric profile should be fitted to a Fano line-shape. As shown in Fig. 2(c), Fano resonance with an asymmetric line-shape with a Q_F of 491 and an ER of 10 dB is achieved.

Additionally, to achieve more insightful information than single device, a sufficiently large amount (30 dies) of PTE-PCNCs with N_{taper} = 30 and g = 600 nm is tested. The average resonance wavelength value is 1532.5 nm. The standard deviations is 8.1 nm, which should be decreased in further study by improving the structure fabrication tolerance. For N_{taper} = 30 and 600 nm, the highest measured Q-factors is 2.41 × 10^4. In average, the Q-factors of the fundamental mode for is about 1.58×10^4. These results indicate that the mass manufacture of high-Q Fano resonance from air-mode PTE-PCNC is feasible by using CMOS-compatible technologies.

IV. Conclusions

In conclusion, an ultra-compact and high Q-factor Fano resonance from air-mode PTE-PCNC structure in SOI platform suitable for DUV lithography is demonstrated. The results will contribute to building ultra-compact lab-on-chip resonance-based photonic components such as sensors, switches, filters, reflectors, and so on.

Acknowledgment

This work is sponsored by National Natural Science Foundation of China (61904196, 62274179, 62235001), National Key R&D Programme (2022YFB2802400).

References

[1] W. Xie, P. Verheyen, M. Pantouvaki, J. Van Campenhout, and D. Van Thourhout, "Efficient Resonance Management in Ultrahigh - Q 1D Photonic Crystal Nanocavities Fabricated on 300 mm SOI CMOS Platform," Laser Photonics Rev., 15(2), 2000317 (2021).

[2] K. Qubaisi, D. Onural, H. Gevorgyan, M. Popović, "Photonic crystal modulator in a CMOS foundry platform." Optical Fiber Communications Conference and Exhibition (OFC). IEEE, (2021).

[3] K. Qubaisi, M. Schiller, B. Zhang, D. Onural, M. Naughton, M. Popović, "Cubic-wavelength mode volume photonic crystal nanobeam cavities in a monolithic CMOS platform." Opt. Lett., 48(4), 1024-1027, (2023).

[4] Y. Xiao, F. Wang, D. Mao, T. Kananen, T. Li, H. Lee, and T. Gu, "Scalable Photonic Crystal Waveguides With 2 dB Component Loss," IEEE Photonics Technology Letters, 34(12), 637-640, (2022)..

[5] D. Dodane, J. Bourderionnet, S. Combrié, and A. Rossi, "Fully embedded photonic crystal cavity with Q= 0.6 million fabricated within a full-process CMOS multiproject wafer," Opt. Express, 26(16), 20868-20877 (2018).

[6] M. F. Limonov, M. V. Rybin, A. N. Poddubny, and Y. S. Kivshar, "Fano resonances in photonics," Nat. Photonics 11, 543‑554 (2017).

[7] Z. Cheng, J. Dong, X. Zhang, "Ultracompact optical switch using a single semisymmetric Fano nanobeam cavity," Opt. Lett., 45(8), 2363-2366(2020).

[8] L. Gu, B. Wang, Q. Yuan, L. Fang, Q. Zhao, X. Gan, J. Zhao, "Fano resonance from a one-dimensional topological photonic crystal," APL Photonics, 6(8), 086105, (2021).

[9] Q. Quan and M. Loncar, "Deterministic design of wavelength scale, ultra-high Q photonic crystal nanobeam cavities," Opt. Express, 19(19),18529-18542 (2011).